13

Modeling the Dynamics of Air Pollutants: Trans-Boundary Impacts in the Mexicali-Imperial Valley Border Region

Alberto Mendoza[1], Santosh Chandru[2], Yongtao Hu[2],
Ana Y. Vanoye[1] and Armistead G. Russell[2]
[1]*Tecnológico de Monterrey, Campus Monterrey,*
[2]*Georgia Institute of Technology,*
[1]*Mexico*
[2]*United States of America*

1. Introduction

Air pollution continues to be an increasing problem in the largest metropolitan areas and regional industrial and commercial corridors in the world. This is also the case in Mexico. Current air quality trends in Mexico indicate that major urban centers continue to exceed the Mexican Ambient Air Quality Standards (MAAQS) for ozone (O_3) and particulate matter with less than 10 microns of aerodynamic diameter (PM_{10}), while other cities are starting to show warning signs of future air quality problems (Zuk et al., 2007). $PM_{2.5}$ monitors are just starting to be deployed around the country, thus no extensive historical data is available on this pollutant.

Some of the urban centers of concern share a common airshed with twin cities across the international border with the United States of America (USA), bringing additional complexity to the study of air pollution dynamics in the region. In this sense, trans-boundary air pollution across USA and Mexico has become a rising problem due to increased commercial and industrial activities in the border region. Trans-boundary air pollution has been studied at different levels in different areas of the border region (Mukerjee, 2001). Two main areas can be identified as the ones that have drawn most of the attention. The first one is the Lower California Area: Tijuana/San Diego, Mexicali/Calexico-Imperial Valley (Figure 1). Here, most of the attention has been on primary PM (e.g., Osornio-Vargas et al., 1991; Chow et al., 2000; Sheya et al., 2000; Kelly et al., 2010), with some studies addressing secondary pollutants (e.g., Zielinska et al., 2001). The second area is the airshed formed by Ciudad Juarez-El Paso-Sunland Park. Perhaps, this area is the one that has received most of the attention regarding trans-boundary air pollution and in a more comprehensive fashion (Currey et al., 2005).

Two of the key steps to improving air quality in a region are identifying, quantitatively, the emissions from sources that affect the area, and assessing how those emissions evolve in the atmosphere to impact pollutant concentrations. Both are difficult, and both can be subject to uncertainties. Air quality modeling is key to both steps because it provides a means to do

Fig. 1. Location of the twin cities of Mexicali-Calexico and Tijuana-San Diego in the Mexico-US border region.

both in a consistent, supportable fashion (Russell & Dennis, 2000). Armed with such information, policy makers can then identify environmentally and economically effective strategies to improve air quality (McMurry et al., 2004).

As indicated, trans-boundary air pollution has been studied at different levels in different areas of the US-Mexico border region. However, limited modeling studies exist where comprehensive chemistry-transport air quality models (CTMs) have been applied at a regional level to understand trans-boundary air pollution in the Mexicali-Imperial Valley border region. In the present study we used a CTM to describe pollutant formation and transport around the Mexicali-Imperial Valley border area, as well as to estimate source contributions to O_3 and $PM_{2.5}$. Even though the principal attention in this study was on the Mexicali-Imperial Valley area, we also expanded our attention outside this area to track down pollutant transport from major urban centers and point sources outside it, but close enough to affect the air quality of the valley (e.g., Tijuana in Mexico, and San Diego and Los Angeles [LA] in the USA).

2. Past air pollution studies in the Mexicali-Imperial Valley Border Area

Tijuana-San Diego has been a border economical belt for a long time. However, over the last 15 years, Mexicali has been one of the fastest-growing cities in Mexico in terms of industrial development, job creation, and energy demand (Quintero-Núñez et al., 2006). This has resulted in that Mexicali on the Mexican side of the border is non-compliant with respect to CO, O_3 and PM_{10} MAAQS, as Calexico is in non-attainment for PM_{10}, $PM_{2.5}$, and O_3 USA standards.

Harmful contaminants in the Mexicali-Imperial Valley border region originate from a number of sources (Sweedler et al., 2003; Quintero-Núñez et al., 2006), including motor vehicles, farms, power plants (natural gas fired and geothermal), and factories. Light manufacturing operations, waste disposal sites, mining, and aggregate handling are also located near the border. In particular, poorly maintained vehicles contribute heavily to the levels of CO, NOx ($NO+NO_2$), and hydrocarbons (HCs) in the air; driving on unpaved roads contributes heavily to PM emissions. Burning of trash, tires, and other materials are also sources of PM, SO_2, and CO.

Several studies have been conducted to understand the composition, spatial variability, and sources of air pollution in the Mexicali-Imperial Valley region. Cerro Prieto, the largest geothermal plant in Latin America (720 MW) is located ~30 km to the south of downtown Mexicali. Since it started operations in the 1970's, H_2S emissions and transport from this facility to Mexicali and Imperial Valley has been a concern (Gudiksen et al., 1980; Deane, 1984). However, atmospheric conversion of H_2S to SO_2 was estimated as not significant. A major effort to understand PM_{10} pollution in Mexicali and Imperial Valley was undertaken in the early 1990's (Chow et al., 2000; Chow & Watson, 2001; Watson & Chow, 2001). This study demonstrated that PM_{10} in the region is mainly composed of crustal material (50% to 62% of the mass) and organic matter (over 25% of the mass). Receptor modeling gave evidence that pollution transport from LA to Mexicali and Calexico could be a concern. In addition, preliminary pollutant flux estimates indicated that the total PM_{10} flux from Mexico to the USA was about 1.5 times the total flux from the USA to Mexico. PM_{10} levels in Mexicali are consistently higher than in Imperial Valley, however wind patterns tend to be in a higher percentage from the north. Other studies have also given evidence of the potential transport of emissions originating in Mexicali and Imperial Valley to areas to the north like the Grand Canyon National Park (Eatough et al., 2001). However, these results have relied on the use of receptor models rather than comprehensive CTMs.

More recently, the fact that the Mexicali Valley and Imperial Valley continue to experience high air pollutants levels made it relevant to conduct an integrated study of the air quality problem in the region. Partial results of this integrated study have been published elsewhere, particularly on levels and chemical composition of fine PM (Mendoza et al., 2010), chemical speciation and source apportionment of VOCs (Mendoza et al., 2009), mobile source emissions characterization using a mobile laboratory (Zavala et al., 2009), and numerical experiments to address the meteorological patterns that foster air pollution episodes (Vanoye & Mendoza, 2009). Here we present our findings on the application of a regional three-dimensional comprehensive CTM to the Mexicali-Calexico border region to follow the dynamics of gas-phase and particulate-phase air pollutants. Particular emphasis is placed on the relevance of understanding trans-boundary air pollutants transport and the implications on emission control strategies on both sides of the border.

3. Description of the modeling system and its application

3.1 Modeling platform

Three-dimensional CTMs continue to be the most scientifically sound tool to assess how emissions from multiple sources impact air quality (Russell & Dennis, 2000). The modeling effort in this study consisted in the application of an advanced air quality and emissions modeling system to the border region to assess how particular sources impact O_3 and $PM_{2.5}$ levels. Specifically, we applied an extended version of the Models-3 suite, including the

Community Multiscale Air Quality model -CMAQ- (Byun & Ching, 1999) for air quality modeling, the PSU/NCAR 5th generation Mesoscale Meteorological model -MM5- (Grell et al., 1995) for meteorological modeling, and the Sparse Matrix Operator Kernel for Emissions model -SMOKE- (Houyoux & Vukovich, 1999) was used to process emissions.

3.2 Modeling domains

The modeling system was applied using nested grids (Figure 2). At the coarser scale, horizontally, 36 km × 36 km grid cells were used. This mother domain is the same as the one defined by the Regional Planning Organizations (RPOs) that oversee other major modeling efforts in North America (i.e., VISTAS, WRAP, CENRAP, LADCO, MANE-VU). At the horizontal mid-resolution level, we included a 12 km × 12 km grid (Figure 3). The coarse grid system allows relatively rapid simulation to set appropriate boundary conditions for the finer grid, serves to stabilize the meteorological and air quality model solutions, and to consider long-range transport from very particular sources. A 4 km × 4 km grid was specified in the Mexicali area for simulations that suggested that fine scale features existed and could not be accurately represented using the coarser grids (i.e., capture the dynamics at the urban scale in Mexicali-Calexico). In this work, we only present the results obtained with the 12 km x 12 km grid, which are ones than provide details on the mid-range pollutants transport in the border region of interest. Details on the extent of each modeling domain are presented in Table 1. The horizontal resolution (including grid nesting) was kept consistent between MM5, SMOKE and CMAQ.

3.3 Episodes selection

The adequate selection of modeling episodes constitutes a fundamental part of the modeling process. If representative episodes are not selected adequately, the modeling results might not characterize effectively the meteorological features that foster high pollution level episodes. Here we used Classification and Regression Tree (CART) Analysis (Breiman et al., 1998) as the formal statistical tool to select the modeling episodes of interest. In essence, CART is a recursive binary partition technique. It divides a set of observations in subgroups taking as reference the value of a particular variable defined by the user (e.g., maximum daily ozone concentration). Each partition in the decision tree is conducted to minimize the classification error of the decision variable. This technique has demonstrated its capacity to help in the selection of days with similar meteorological conditions that give rise to similar pollution levels, using a formal procedure and eliminating the effects of meteorological variability (Kenski, 2004).

CART was applied to obtain decision trees to classify daily maximum O_3, CO and PM_{10} concentrations (separately). The database used was composed of observations (chemical and meteorological) taken by air quality stations in the border region for the years 2001 and 2002. The purpose was to group days with similar O_3, CO, and PM_{10} levels and influenced by similar meteorological condition. The results obtained from CART application were compared against time series plots to corroborate that the episodes selected in fact represented a continuum of days with relatively high pollutant concentrations levels. One of the parameters that can be manipulated while applying the CART technique is the number of final bins that the decision tree will have. Typically, as the number of bin increases the error is reduced; however, if the number of bin increases the probability of having consecutive days in a bin decreases and thus it is harder to construct episodes for air quality

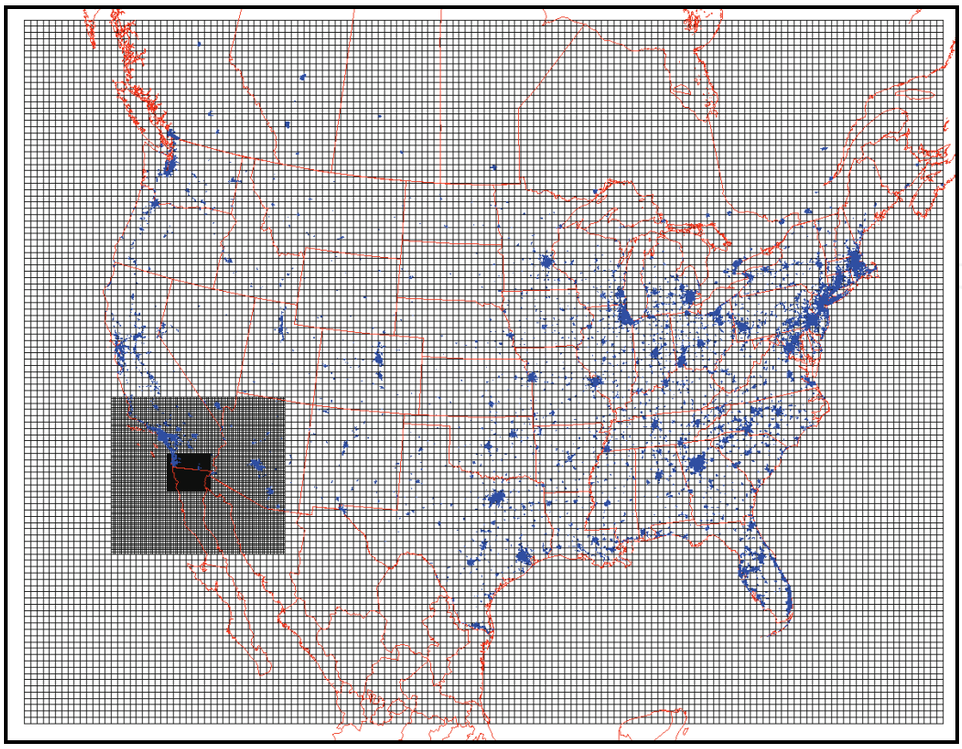

Fig. 2. Horizontal resolution of the nested modeling domain.

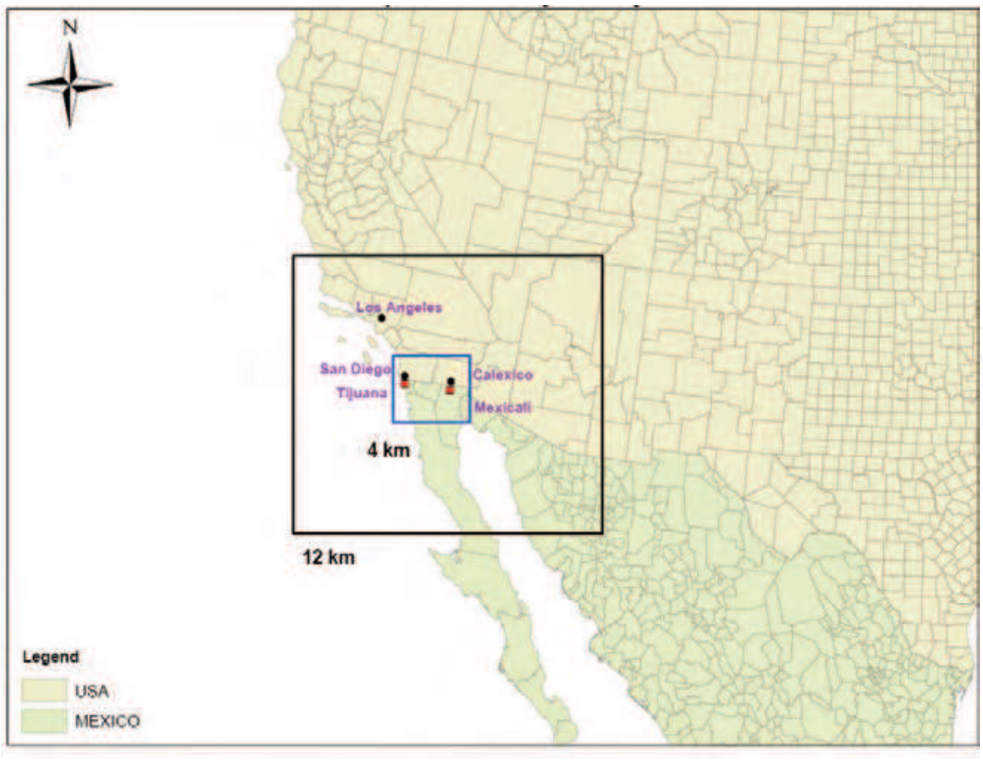

Fig. 3. Location of the 12 km and 4 km horizontal modeling domains.

Grid ID	Origin (x, y) in km	Horizontal domain (# columns, # rows)
USMEX36	(−2736.0, −2088.0)	(148,112)
USMEX12	(−2232.0, −1160.0)	(84,75)
USMEX4	(−1908.0, −756.0)	(63,54)

Table 1. Modeling domains specifications. Origin coordinates are based on a Lambert Conformal Conic projection with centre lat. and long. as 40 and −97 degrees, respectively

modeling purposes. A convenient number of consecutive days for a modeling episode is between 10 and 15, so with this in mind the number of bins was varied until decision trees with low classification errors and high number of consecutive days in the bins were obtained.

Based on the CART Analysis application, the following modeling episodes were defined: August 18-27, 2001 and July 17-25, 2001 for high O_3 events, and January 6-16, 2002 for high CO and PM events that are typical during autumn and winter times. Additional details on the episode selection process can be found elsewhere (Vanoye & Mendoza, 2009).

3.4 Emissions modeling

SMOKE is a computational engine used to generate the gridded emissions inventory, and its main purpose is to speciate and allocate spatially and temporally area and point emissions and to couple emission estimation tools for mobile and biogenic emissions to spatial and temporal allocation routines.

Base emissions inventory data for the USA side of the border were obtained from the 2001 US National Emissions Inventory (NEI) prepared for the Clean Air Interstate Rule (CAIR). Emissions for the Mexican side came from combining the 1999 BRAVO Mexican inventories (Pitchford et al., 2004) with the 1999 Six Border States Mexican inventory (MNEI) (ERG et al., 2004). Biogenic emissions for both sides of the border were prepared using BEIS3 (Vukovich & Pierce, 2002), and USA mobile emissions were prepared using MOBILE6 (US EPA, 2003). Mobile emissions for Mexico were directly obtained from BRAVO and MNEI.

The emissions inventory generated considers O_3 and PM precursors, as well as primary PM emissions and some toxics (particularly VOC species). The modeling episodes selected were not the same ones as the base years used to derive the raw emissions inventories used for the Mexican side of the border; thus, scaling was needed to update the emissions (e.i., MNEI base year is 1999 and modeling years for our applications were 2001 and 2002). This scaling was based primarily on population growth. VOCs speciation was conducted based on the chemical mechanism selected for the CTM application: SAPRC-99 chemistry (Carter, 2000). Spatial surrogate ratios used to allocate emissions on both sides of the border considered population, highways, total railroads, airport points, and marine ports.

As an example of the results obtained from the application of SMOKE, Figure 4 illustrates CO and biogenic isoprene emission inventories for the 12 km resolution domain. It can be seen, for example, that the CO emissions inventory contains the expected spatial structure (main roads are clearly shown and emissions follow general population patterns). Overall, mobile sources contribute to ~65% of the NOx and ~30% of the VOCs emitted in the LA area; area sources represent ~15% of the NOx and 25% of the VOCs emitted in LA. Values for San Diego are similar as the ones for LA. In contrast, 34% of the NOx and 13% of the VOCs emitted in Mexicali come from mobile sources; area sources (including non-road

mobile sources) represent 37% of the NOx and 51% of the VOCs emitted in Mexicali. In Tijuana, mobile sources emit 61% of the NOx and 23 of the VOCs, whilst area sources emit 29% of the NOx and 60% of the VOCs. PM in the Mexicali-Calexico region comes from area sources that are dominated by wood-fuel combustion, agricultural burning, and paved and unpaved road dust.

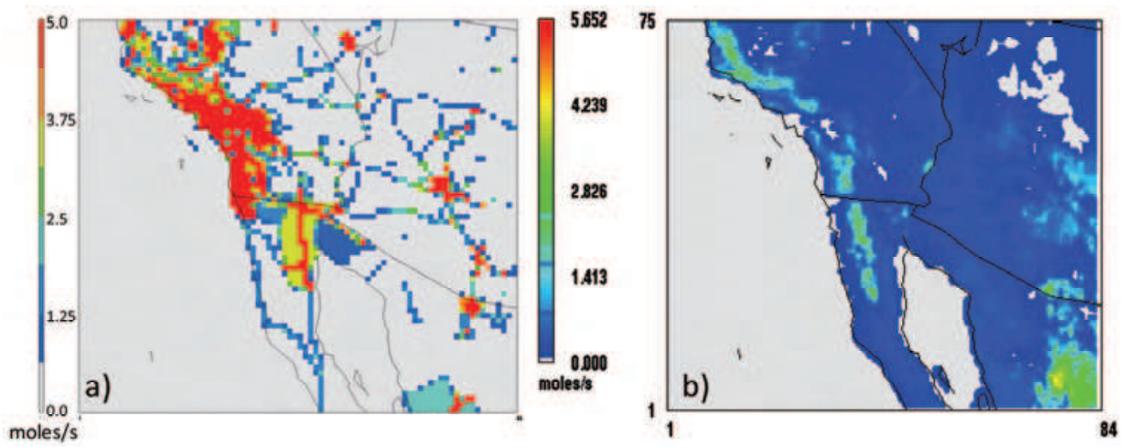

Fig. 4. Examples of (a) CO and (b) biogenic isoprene emissions allocated in the 12 km resolution modeling domain.

3.5 Meteorological modeling

MM5 (Grell et al., 1995) version 3.7 was the meteorological model used here to develop the fields needed to drive the CTM simulations and to provide meteorological information needed to estimate meteorological-variable emissions (e.g., biogenic emissions depend on solar radiation and temperature, while mobile emissions depend on temperature). MM5 is a non-hydrostatic mesoscale meteorological model with grid nesting and four-dimensional data assimilation capabilities. Here we briefly describe the model setup and the input data used to run the model. Additional details, including model performance statistics on the MM5 application, can be found elsewhere (Vanoye & Mendoza, 2009).

MM5 was run with 34 vertical layers with the top of the domain set at 70 mb; horizontal resolution was described earlier. Following a set of sensitivity tests, the MM5 parameterization configuration that gave the best statistical performance of the model for the July and August episodes is presented in Table 2. Of note, the Pleim-Xiu Land Surface model is the recommended scheme by the US Environmental Protection Agency (US EPA) and is the one that has demonstrated to give the best meteorological fields for CMAQ (Olerud & Sims, 2003; Morris et al, 2004). Another advantage of the Pleim-Xiu scheme is that it allows using CMAQ's dry deposition scheme which is technically superior to the conventional Wesley scheme.

MM5 was executed enabling its four-dimensional data assimilation capabilities for the 36 km and 12 km domains. One-way nesting was selected as the way MM5 transferred information from the outer grids to the inner grids. Finally, a relaxation scheme was chosen for the manipulation of the boundary conditions, i.e. the five outermost points are used to damp the information flowing from the boundaries to the inner domain.

Initial and boundary condition were prepared using the National Center for Atmospheric Research (NCAR)/National Centers for Environmental Prediction (NCEP) Eta analyses

data. The data consist of regional meteorological analyses for North America based on the output of the Eta model, which generates data every 12 hours from observations of over 600 stations in the region. To complement this information and increase the effectiveness of the data assimilation step, additional observations with a temporal resolution of 6 hours were extracted from NCAR archives, through its Data Support Section of the Scientific Computing Division. This included observations from surface and marine stations, as well as from aerial soundings. Basic landuse, vegetation cover and topography was also obtained from NCAR. Landuse information was based on the USGS 24 categories, and topographic resolutions of 10 min, 5 min, 2 min, and 30 sec were used.

Parameter ID	Description	Selected option
IMPHYS	Explicity Moisture Scheme	Mix Phase
MPHYSTBL	Intrinsic Exponent for Calculating IMPHYS	Use Look-up table for moist physics
ICUPA	Cumulus Schemes	Grell
IBLTYP	Planetary Boundary Layer	Pleim-Xiu
FRAD	Radiation Cooling of Atmosphere	Rapid Radiative Transfer Model
ISOIL	Multilayer Soil Temperature Model	Pleim-Xiu Land Surface Model
ISHALLO	Shallow Convection Option	No Shallow Convection

Table 2. MM5 parameterization options that gave the best model performance for the simulation of meteorological conditions in the Mexicali-Imperial Valley border area.

3.6 CMAQ application

3.6.1 Base case simulations

CMAQ is an Eulerian photochemical model that simulates the emissions, transport, and chemical transformations of gases and PM in the troposphere (Byun & Ching, 1999). Similar to other photochemical models, CMAQ solves the species conservation equation:

$$\frac{\partial C_i}{\partial t} = -\nabla \cdot (\mathbf{u} C_i) + \nabla \cdot (\mathbf{K} \nabla C_i) + R_i + E_i \quad (1)$$

where, C_i is the concentration of species i, $\mathbf{u}$ is the wind field, $\mathbf{K}$ is the eddy diffusivity tensor, R_i is the net rate of generation of specie i, and E_i is the emission rate of species i. Meteorological parameters such as $\mathbf{u}$ and $\mathbf{K}$ in eq. 1, as well as temperature and humidity fields come from the MM5 application, while emission rates from SMOKE. CMAQ contains state-of-the-science descriptions of atmospheric processes and has a "one-atmosphere" approach for following the dynamics of gas-phase and particulate matter pollutants. The latter is an important characteristic to assess simultaneously O_3 and aerosols.

CMAQ, as MM5, allows for grid nesting. The horizontal grid structure used was described earlier. The vertical structure of all domains has 13 layers with its top at about 15.9 km above ground. Seven layers are below 1 km and the first layer thickness is set at 18 meters.

Initial and boundary conditions used for the mother domain were the same as the ones suggested by other RPO applications (Russell, 2008). Results from the simulations were compared to data from ground-based monitors for NO_2, O_3, CO, SO_2, PM_{10}, and $PM_{2.5}$. Observational data was obtained from the California Air Resources Board (CARB) for

monitoring stations in the State of California, and from Mexican border municipalities of interest (i.e., Tijuana and Mexicali). Observational data were also obtained from US EPA's Air Quality Data system. In each episode, the first two days were considered ramp-up days and were not further used for additional analysis.

CMAQ has been used extensively to study air pollutant dynamics in the continental USA (e.g., Tagaris et al., 2007; Liao et al., 2007) and in particular regions of that country (e.g., Dennis et al., 2010; Ying & Krishnan, 2010), as well as in other countries around the world (e.g., Che et al., 2011; Im et al., 2011). Only one additional application using CMAQ as the CTM has looked at trans-boundary air dynamics in the USA-Mexico border using fine scale grid resolutions. Choi et al. (2006) looked at high PM events over the sister cities of Douglas, Arizona (USA) and Agua Prieta, Sonora (Mexico). In that application, model performance was acceptable, and it was concluded that secondary processes contributed marginally to the modeled PM events. Primary local sources dominated high PM events.

3.6.2 Sensitivity analysis

Sensitivity analysis is an important tool that can be used to understand the impacts of emissions from various sources on ambient air concentrations of specific pollutants. The ability to conduct sensitivity analyses in an efficient fashion is critical to obtain robust descriptions of the response fields of pollutant concentrations to changes in model inputs (particularly emissions), which then are used in source attribution analyses and control strategy design (e.g., Bergin et al., 2007). Among the different choices to estimate the sensitivity fields, the direct decoupled method for three-dimensional models (DDM-3D) has proven to be superior to other techniques (Yang et al., 1997; Hakami et al., 2003). DDM-3D is an implementation of the Decoupled, Direct Method (Dunker, 1984; Dunker et al., 2002) for sensitivity analysis. The version of CMAQ used in our applications was extended with DDM-3D (Cohan et al., 2005). The method directly calculates the response of model outputs (concentrations) to parameters and inputs, i.e., the semi-normalized sensitivities S_{ij}:

$$S_{ij} = \frac{\partial c_i}{\partial e_j} \tag{2}$$

where c_i is the concentration of species i and e_j is the relative perturbation on parameter j –p_j- (e.g., NOx emissions) from its nominal value $p_j°$ (i.e., $e_i = p_j/p_j°$). This is an efficient approach for directly assessing the sensitivity of model results to various inputs and parameters, and replaces the need to use the traditional brute force approach of re-running a model after modifying a parameter. More importantly, it does not suffer from numerical noise problems that can overwhelm brute force approaches. In addition, it is a linear method. In prior studies, the atmospheric chemistry has been found to respond relatively linearly for emissions changes on the order of 25% or more (Dunker et al., 2002; Hakami et al., 2004).

Of particular interest was to explore the sensitivity due to variations on the emissions inventory. The implementation of DDM to CMAQ allows defining spatial- and source-specific emissions categories as the input being perturbed, and in a single model run the sensitivities of all species tracked by the model to changes in a set of emissions sources can be calculated. To accomplish this, the region of interest was divided into three different areas: Mexicali-Calexico (abbreviated as MXC), Tijuana-Tecate-San Diego (abbreviated as

TSD), and Los Angeles-Riverside-Orange-Ventura (abbreviated as LAR). O_3 sensitivities to area-, mobile-, and point-source emissions of NOx and VOC were calculated for each of the regions defined for both summer episodes. Additionally, $PM_{2.5}$ sensitivities to changes in the same source categories were calculated.

4. Results

4.1 Air quality model performance

Domain-wide episode performance statistics were determined to ascertain the confidence of the simulation results. Table 3 presents the average model performance for the 12 km domain in terms of Mean Bias Error (MBE), Root Mean Squared Error (RMSE), Mean Normalized Bias (MNB), and Mean Normalized Error (MNE). Established performance guidelines indicate that the model should have a MNB of ±5–15%, and a MNE 30–35% for O_3 (Tesche et al., 1990). Based on these guidelines, CMAQ performed well in predicting the observed O_3 concentrations. No guidelines exist for the rest of the gas-phase species, though the results are comparable to results obtained by others using different CTMs (e.g., Mendoza-Dominguez & Russell, 2001). Overall, the gas-phase species results indicate a tendency of the model to underestimate the pollutant concentrations. This is in line with the results obtained from mobile laboratory measurements that indicate an underestimation of the official emissions inventory for Mexicali (Zavala et al., 2009). PM proved to be more difficult to simulate correctly, which is a known setback of current CTMs (Russell, 2008).

		MBE	RMSE	MNB (%)	MNE (%)
August-01	**O_3**	−1.64E-03	1.60E-02	−0.21	19.7
	CO	−3.52E-01	6.56E-01	−18.6	63.2
	NOx	−1.25E-02	2.52E-02	−34.9	74.2
	SO_2	−1.40E-03	5.40E-03	−19.4	87.7
	$PM_{2.5}$	−6.76E+00	9.14E+00	−36.9	39.2
	PM_{10}	−3.00E+01	3.57E+01	−76.2	76.2
July-01	**O_3**	−9.19E-02	1.76E-01	−18.3	61.2
	CO	−1.43E+00	1.97E+00	−22.0	56.8
	NOx	−6.18E+00	7.58E+00	−31.0	60.0
	SO_2	−5.31E+00	6.53E+00	−29.2	60.2
	$PM_{2.5}$	−7.10E+00	8.72E+00	−33.3	63.0
	PM_{10}	−8.12E+00	9.97E+00	−35.3	59.5
January-02	**O_3**	2.86E-03	7.76E-03	7.0	14.1
	CO	−7.33E-01	1.33E+00	−26.5	73.1
	NOx	−3.99E-02	7.98E-02	−34.6	76.0
	SO_2	−1.10E-03	5.40E-03	−29.6	74.4
	$PM_{2.5}$	−2.54E+00	1.01E+01	−4.6	37.2
	PM_{10}	−2.53E+01	3.21E+01	−56.1	61.7

Table 3. Average performance metrics for the 12 km domain during the diferent episodes modeled. MBE and RMSE are in ppmv for gas-phase species and μg/m^3 for PM species.

Peak O_3 concentrations in Calexico during the August episode were observed at Ethel Street (MBE –4.0 ppbv, MNB –3.0%), and East Calexico (MBE 5.0 ppbv, MNB 12.0%) sites. Calexico and Mexicali, being adjacent to each other in the border region, experience similar O_3 concentrations. The inability to capture the minimums in Ethel Street and Calexico East sites can be attributed to the fact that both these locations are located close to roadways, hence experience strong O_3 sinks in the night time due to its reaction with NO which the model is unable to capture using the 12 km grid structure (Figure 6).

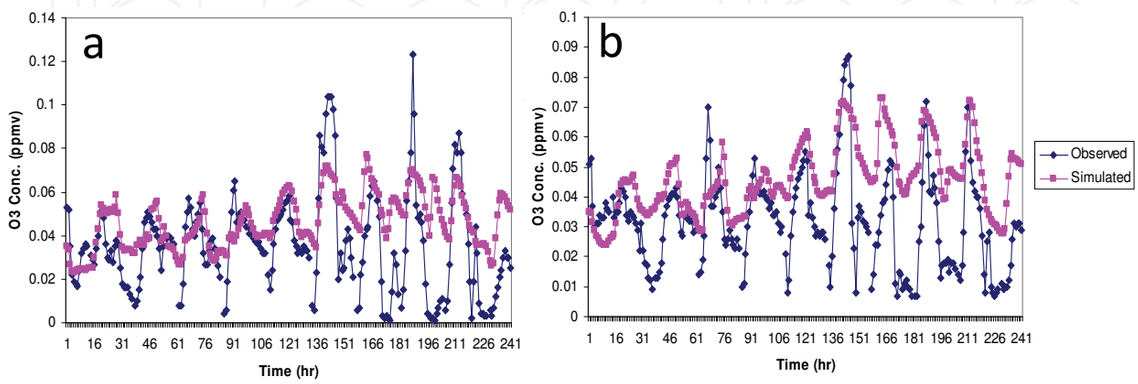

Fig. 6. Observed vs. simulated O_3 concentrations at representative sites in Calexico during August 2001 at (a) Ethel Street and (b) Calexico East site. Time scale represents hours of simulation.

Also, the LAR area was tested for model performance with respect to spatial as well as temporal variability (Figure 7). This region was chosen because of the high density of monitoring stations located in it, which can give a more realistic comparison with the modeled average hourly concentration values in the region. During the August episode, the peak O_3 concentrations occurred on August 26th, 2001: 189 ppbv at the Azusa site and 190 ppbv at the Glendora Laurel station, respectively. These sites are located in the San Gabriel Valley and come under the same 12 km grid cell. Simulated concentrations correlated well with the observed concentrations at Azusa (MBE 5.0 ppbv, MNB 12.2%) and Glendora Laurel (MBE 0.0 ppbv, MNB 3.5%) on most days. For the January episode, January 12 and 13, 2001 were the high concentration days with peaks of ~60 ppbv in the Los Angeles area, and ~75 ppbv in the Mexicali area.

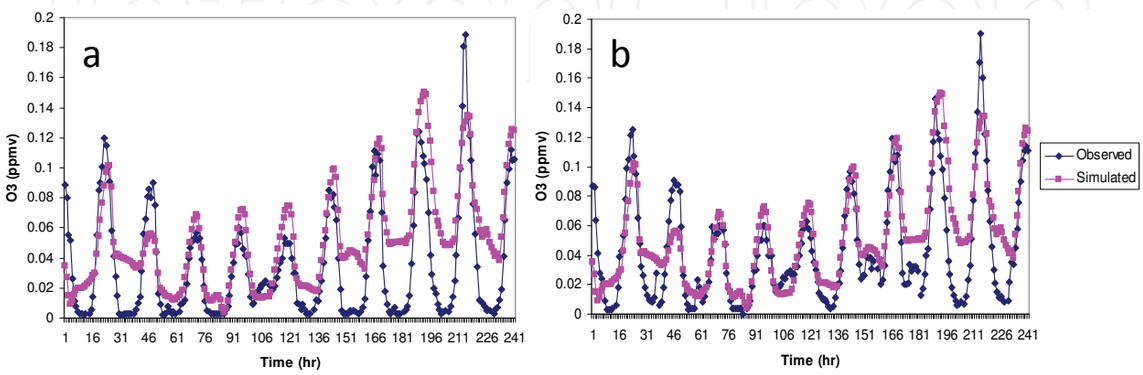

Fig. 7. Observed vs. simulated O_3 concentrations at representative sites in LA, during August 2001 at (a) Azusa, (b) Glendora Laurel. Time scale represents hours of simulation.

4.2 Modeled pollutant concentration fields

Resulting O_3 fields for the July and August episodes illustrate the influence of regional transport across the domain. During the July 2001 episode, a peak of 125 ppbv O_3 was simulated in the LA area on July 23, 23:00 hrs UTC (Figure 8d). The plume from LA can be seen transported towards the east (Figure 8 a-c). Plumes of up to 78 ppbv O_3 emerge from San Diego-Tijuana and travel eastwards and reach the Mexicali-Calexico region (Figure 8 a-c). Peak $PM_{2.5}$ concentrations of over 50 µg/m^3 were simulated in the LA area on July 15th, while $PM_{2.5}$ concentrations did not exceed 15 µg/m^3 in Tijuana-San Diego and Mexicali-Calexico during the July episode.

On August 24th (20:00 hrs UTC), strong O_3 plumes started to develop, and plumes from Mexicali-Calexico and Los Angeles almost converged (Figure 9a). At the same time plumes from Tijuana-San Diego build up as well and move eastwards towards Mexicali-Calexico (Figure 9b). Similar patterns start to emerge on August 25th (19:00 hrs UTC) (Figure 9c); peaks reach 162 ppbv in the LA area on August 26th (00:00 hrs UTC) (Figure 9d). A peak concentration of 162 ppbv is reached about 30 km northwestfrom the Glendora Laurel site where a simulated peak of 144 ppbv is reported. Similar to the July episode, O_3 plumes from San Diego-Tijuana border area are transported eastward towards Mexicali-Calexico during the August episode as well. Peak $PM_{2.5}$ concentration of 100 µg/m^3 are seen close to the LA area on August 25th. In the Mexicali-Calexico region, Mexicali showed a peak of 42 µg/m^3 on August 25th (14:00 hrs UTC).

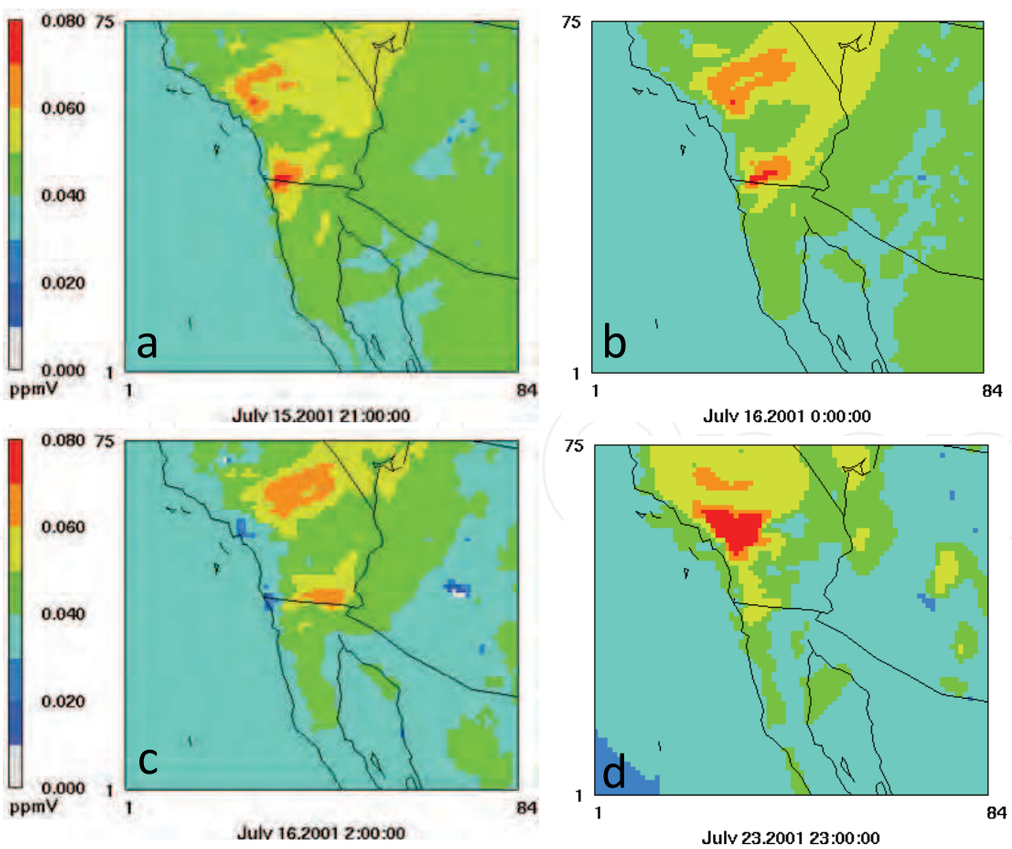

Fig. 8. Regional dynamics of O_3 plumes during the July 2001 episode (see text for details).

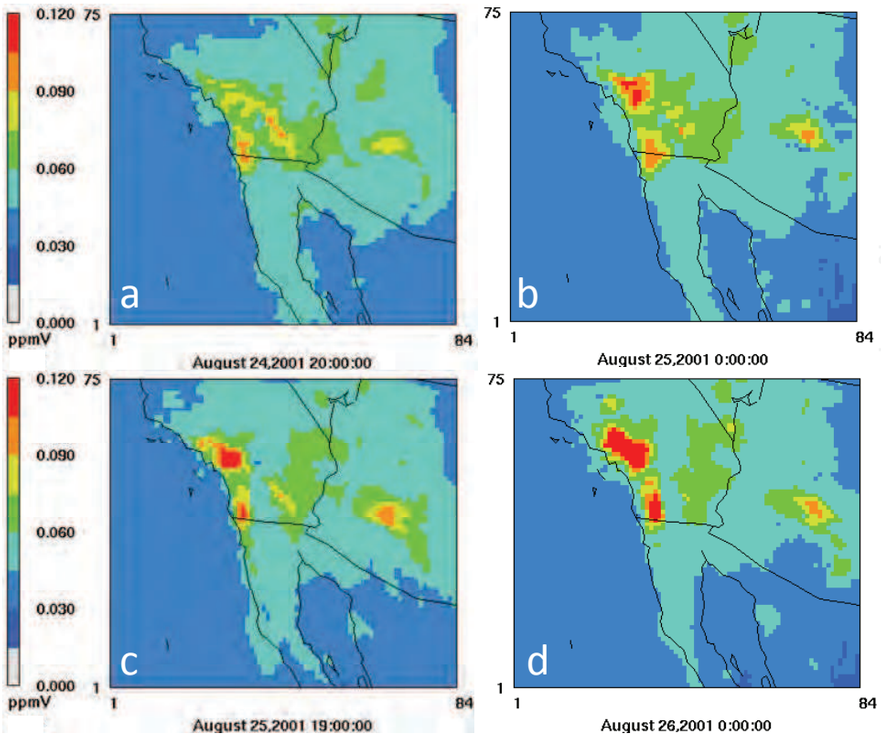

Fig. 9. Regional dynamics of O_3 plumes during the August 2001 episode (see text for details).

In addition to O_3, the dynamics of other primary (e.g., CO, NO_2, and SO_2) and secondary PM species (e.g., sulfate in fine PM) are also of interest when analyzing the output data obtained from CMAQ (Figure 10). For the August episode, CO concentrations peak around 7 PM (PDT), with LA showing the highest concentration, followed by San Diego-Tijuana. CO levels in Mexicali-Calexico are lower and more localized. In general, NO_2 distribution is very similar to that of CO, highlighting the importance of mobile source emissions. SO_2 emissions are highest in the Tijuana region. Thus, with the wind blowing in the northeast direction during the morning hours, much of the SO_2 is transported inland into the San Diego region. Consequently, the sulfate aerosols have a high regional effect encompassing the whole of San Diego region, and also showing its effect on Imperial Valley and Mexicali during late evening hours.

As PM concentrations are a major concern during the winter season, we limit our discussion of the January 2002 episode to $PM_{2.5}$. A peak of 188 µg/m^3 was simulated on January 12, 2002 (18:00 hrs UTC) near LA. The movement of regional $PM_{2.5}$ plumes is represented in Figure 11. Plumes from San Diego-Tijuana, LA and Las Vegas move towards the Mexicali-Calexico region with impacts of 10 to 35 µg/m^3. $PM_{2.5}$ originated in the USA and transported to Mexicali-Calexico, along with local fresh emissions, is carried further southeast inside Mexico. Mexicali-Calexico shows peak $PM_{2.5}$ concentration of 50 µg/m^3. Primary organic mass was the main contributor to fine PM in LA (98 µg/m^3). The maximum contribution from primary organic matter to the fine PM in Mexicali-Calexico was 10 µg/m^3. Peak soil dust concentrations of 40 µg/m^3 were found in Pheonix and Las Vegas areas. The soil dust contributions from LAR, TSD and MXC range between 5-25 µg/m^3 (Figure 11).

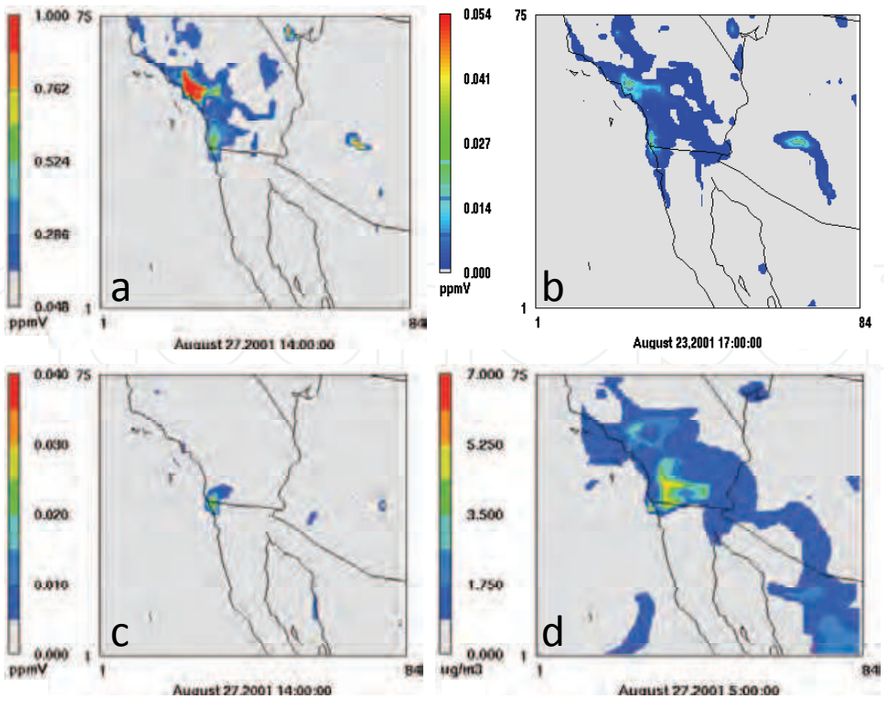

Fig. 10. Concentration fields for gas-phase and aerosol species (August 27, 2001): a) CO, b) NO_2, c) SO_2, d) sulfate $PM_{2.5}$.

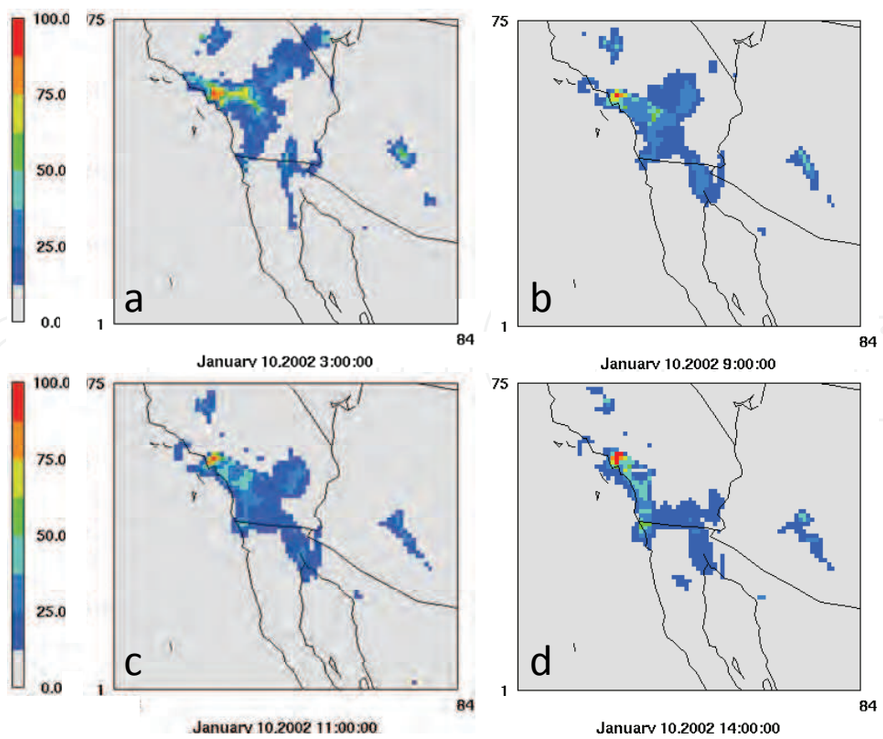

Fig. 11. Dynamics of $PM_{2.5}$ plumes during the January 2002 episode (see text for details).

4.3 Source contribution

4.3.1 Source contribution to specific NOx and VOC emission sources: August episode

To understand source contributions in the modeling domain, sensitivity fields were estimated using CMAQ/DDM. Results are presented only for the August 2001 episode; values for the July 2001 episode were similar. First, the sensitivity of the regional O_3 field to changes in NOx or VOC emissions from specific sources is presented. The figures presented are "response surfaces" and are interpreted as the amount of increment in pollutant concentration per 10% increase in emissions (or amount of reduction per 10% decrease in emissions) from certain source. The sensitivity coefficients are linear (first order) in nature and thus can be used in the manner described. In general, is reasonable to imply a linear response over a range of emissions perturbations (±30%) even for species that it is well known their non-linear response in the atmosphere (e.g., O_3; Hakami et al., 2003).

The impact of NOx emissions from MXC was the highest on August 26, with sensitivity response reaching 9 ppbv of O_3 per 10% change in the emissions (Figure 12). The area of influence of NOx emissions extends northwards into Imperial Valley, and partially into Arizona. The results indicate that down-wind the atmosphere is not NOx-inhibited; that is, an increase in NOx does not give as a response a decrease in O_3 down-wind as has been the case in other areas of the Mexico-US border (Mendoza-Dominguez & Russell, 2001). Change in VOC emissions from sources in MXC produce a smaller change –localized– in O_3 concentrations (maximum of 3 ppbv per 10% change), indicating the benefits of NOx control over VOC control in the region.

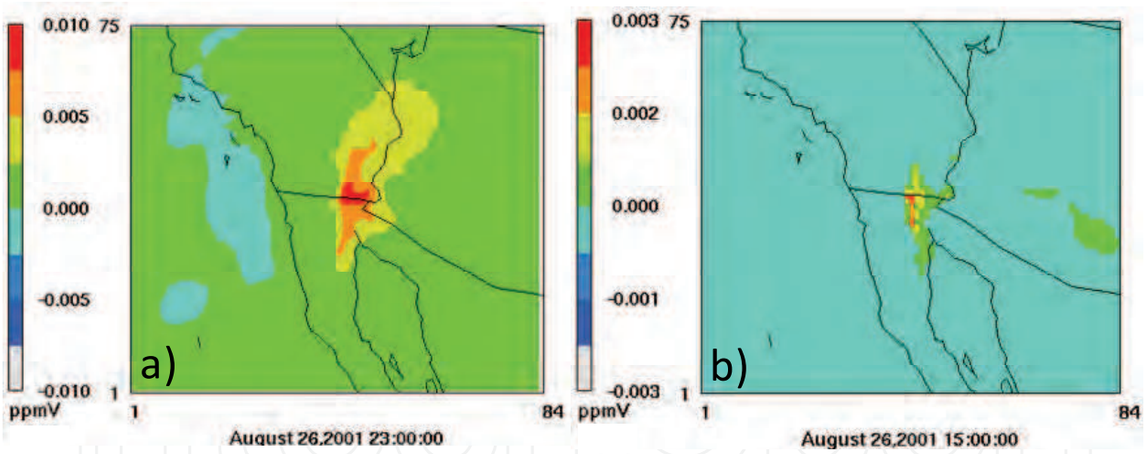

Fig. 12. Maximum sensitivity of O_3 to (a) NOx emissions and to (b) VOC emissions from the MXC region during the August 2001 episode.

The influence of emissions from other geographic locations was also tested. Figure 13a illustrates the response of O_3 to changes in NOx emissions from mobile sources located in the TSD area. The highest impact is almost 17 ppbv, occurring near San Diego, with a strong influence in the MXC region as well. This result indicates that emission controls implemented in San Diego (or increment in emissions) will impact the MXC area accordingly. Of interest is also the small NOx-inhibited region located down-wind of San Diego, toward the Tijuana border, that implies that a decrease in mobile emissions will result in an increase in O_3 concentrations. In contrast, and as expected, impact from VOCs

emitted by mobile sources located in the TSD area is limited to less than 2 ppbv per 10% change in emissions (Figure 13b). The spatial extent of influence is also more limited than the sensitivity to NOx emissions, influencing the northern region of Imperial Valley County.

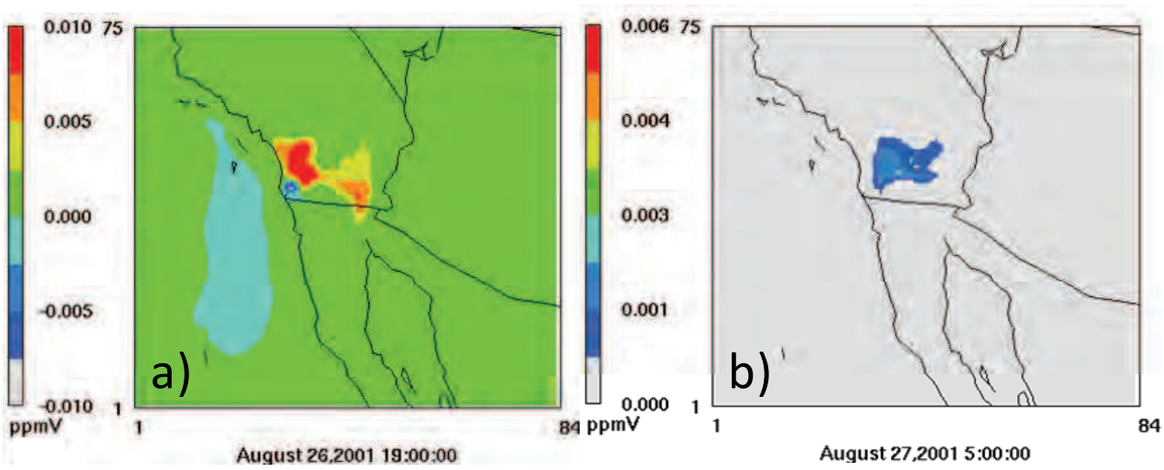

Fig. 13. Maximum sensitivity of O_3 to (a) mobile NOx emissions and to (b) mobile VOC emissions from the TSD region during the August 2001 episode.

Finally, example sensitivity values due to changes in NOx emissions from mobile and area sources from the LAR region are presented (Figure 14). For the case of mobile sources, the increment of NOx emissions results in a decrease in ozone (~7.5 ppbv per 10% increase in emissions) in downtown LA, with a corresponding increase (~30 ppbv) in neighboring counties of Ventura, Orange, and Riverside. From the extent of the sensitivity field, it is possible that under the right meteorological conditions, the influence can reach the Imperial Valley area. On the other hand, the sensitivity to area source NOx is smaller in value and extent because area emissions are smaller than the mobile emissions in Southern California.

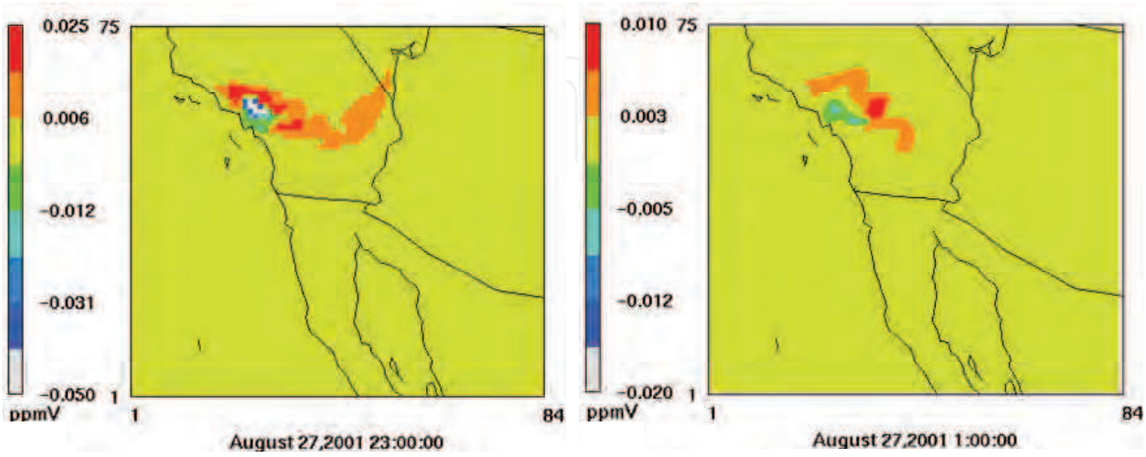

Fig. 14. Maximum sensitivity of O_3 to (a) mobile NOx emissions and (b) area NOx emissions located in the LAR area during the August 2001 episode.

4.3.2 Source contribution to overall emission sources: August episode

When considering the overall emissions from mobile sources, the LAR area made an overall contribution of 44 ppbv on the surrounding region i.e., east of the city of LA towards Glendora Laurel and Azuza on August 26 (00:00 hrs UTC) (Figure 15c). Presence of high concentrations of NOx results in negative sensitivities up to –46 ppbv in urban LA (Figure 15a). As seen in the base case simulations where O_3 plumes from LAR, MXC and TSD formed a triangle over southern California, the O_3 sensitivity fields extends towards MXC with increments of up to 10 ppbv (Figure 15a). Due to the northeasterly direction of the winds, plumes also reach the Grand Canyon National Park area, again with increments of about 10 ppbv (Figure 15d). LAR area sources contribute up to 8 ppbv of O_3 in the Riverside area.

Mobile traffic passing through Mexicali's border crossings is of concern. However, the overall mobile contribution to O_3 is found to be small in the simulation results. The impact from Mexicali vehicles alone is very small, with a peak impact of only 1.3 ppbv over Calexico and Mexicali (Figure 16a). Possible emission inventory underestimates can be a potential reason for low simulated impacts, and should be further explored.

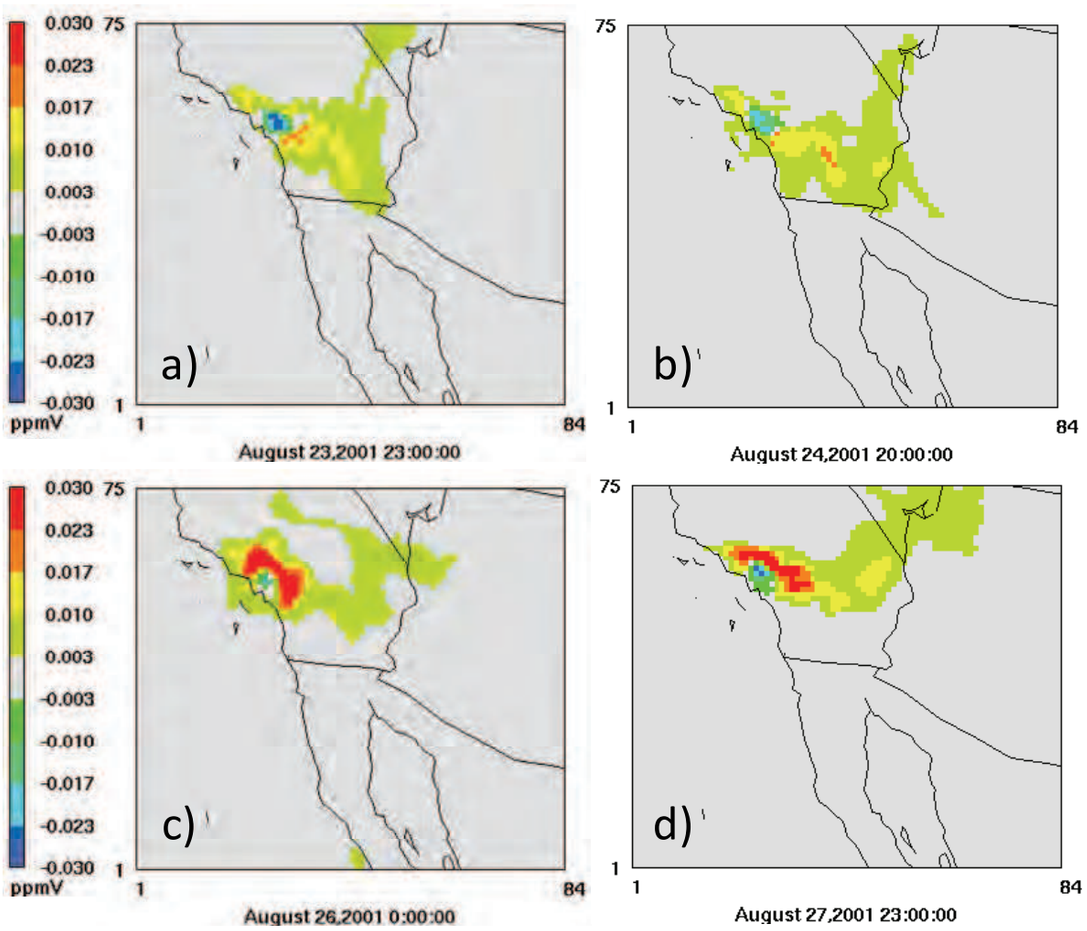

Fig. 15. O_3 sensitivity to LA mobile source emissions (see text for details).

The maximum impact from Calexico mobile sources is 2 ppbv of O_3 seen over the Calexico region itself, and the border between California and Arizona (Figure 16b). The primary areas of mobile emissions are the two border crossing areas (seen in blue as negative sensitivities). Area sources in MXC contribute a simulated maximum of 8 ppbv O_3 during the summer episode (Figure 17a). The area of influence can be seen encompassing California, and the border regions of California-Arizona. O_3 impacts up to 4 ppbv in the Grand Canyon area can be attributed to area sources in the Mexicali-Calexico region (Figure 17b).

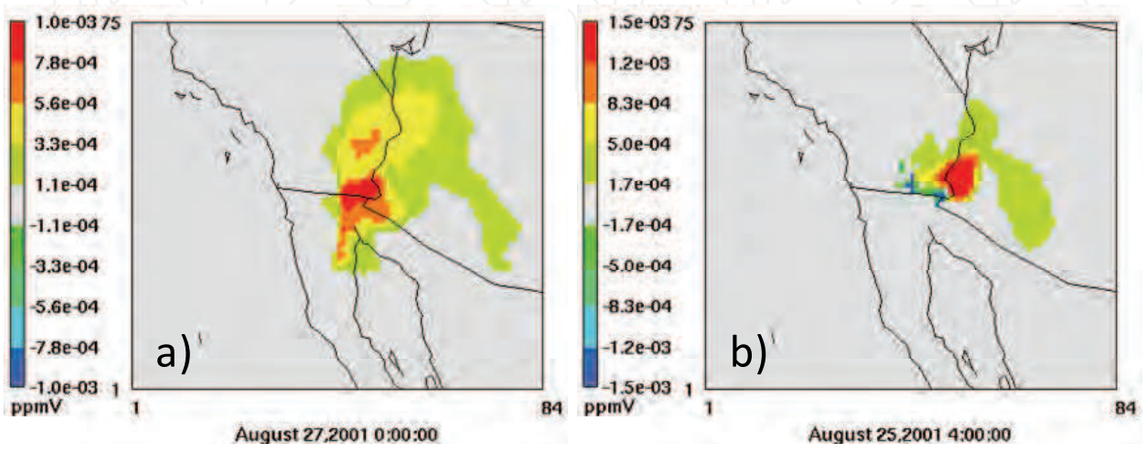

Fig. 16. Contribution to O_3 concentrations from (a) Mexicali and (b) Calexico mobile sources.

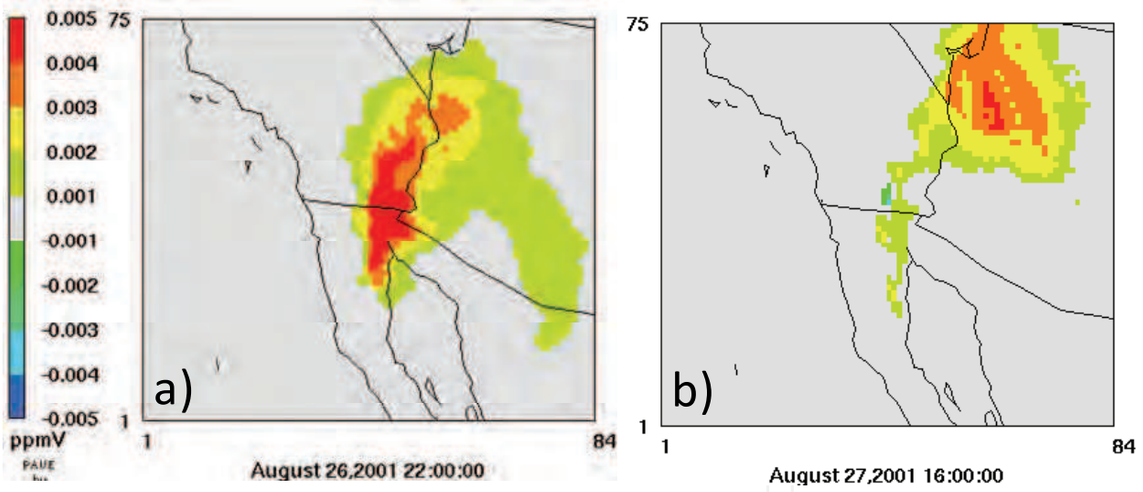

Fig. 17. Contribution to O_3 concentrations from MXC area sources (see text for details).

Area sources from TSD have a peak impact of 40 ppbv of O_3 over the San Diego area and this plume is carried eastwards into the USA close to the border region. The contribution of Tijuana emissions extends to the southeast into inner Baja California and impacting up to 20 ppbv of O_3 (Figure 18a,b). Also, on August 26th, the sensitivity field of O_3 from the TSD region extends eastwards towards Calexico, thus adding O_3 to the already polluted air in Calexico and Mexicali (Figure 18c,d).

Tijuana mobile source impacts reach up to 6 ppbv on both sides of the border depending on the wind direction (Figure 19b,c). Since the dominant wind pattern is towards the northeast,

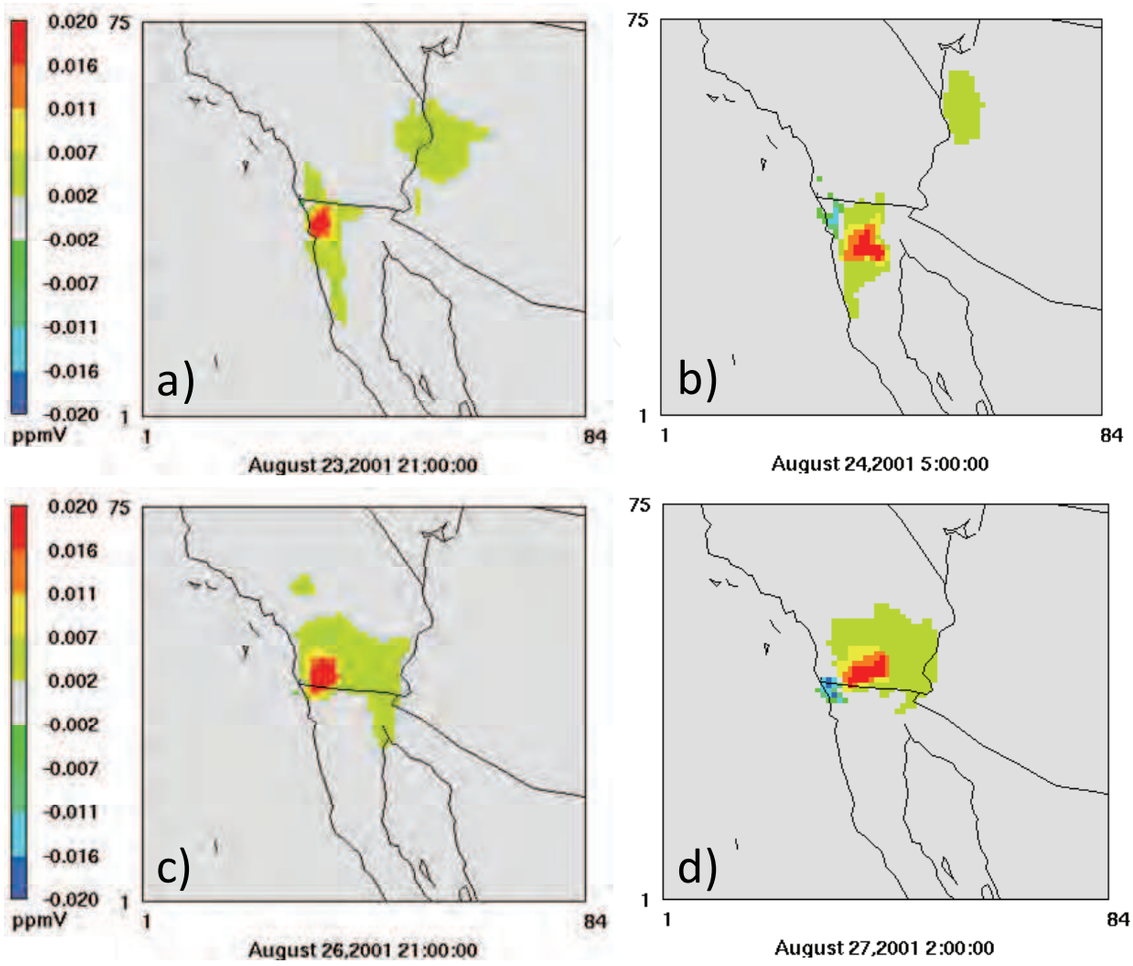

Fig. 18. O_3 sensitivity to TSD area sources during the August 2001 episode (see text for details).

O_3 is transported through the California-Baja California border towards Calexico (Figure 19a,c). Tijuana mobile sources impacts up to 3 ppbv of O_3 in Mexicali-Calexico (Figure 19a). It is also of interest the areas of negative sensitivity observed in downtown Tijuana of more than 3.0 ppbv.

Mobile sources from San Diego contribute up to 26 ppbv of O_3 in the region itself, and also over the park areas such as Anza Borrego Desert State Park located southeast of San Diego (Fig. 20a). The base case scenario showed O_3 plumes from TSD area transported to Mexicali-Calexico. A contribution of up to 11 ppbv of O_3 in Mexicali-Calexico can be attributed to the high density of vehicles in and around the San Diego region (Fig. 20b). This contribution is higher than the contribution from MXC mobile sources.

The peak $PM_{2.5}$ concentration simulated over the MXC region was 42 µg/m^3. Of this, MXC area sources contributed to 21 µg/m^3 of primary $PM_{2.5}$. Thus, 50% of the $PM_{2.5}$ levels in MXC can be attributed directly to MXC area sources during August 2001. $PM_{2.5}$ contribution from MXC mobile sources was very small, with peak contributions less than 1 µg/m^3. MXC point sources contributed the remaining share of up to 7 µg/m^3. Simulations found similar results for TSD with contributions of up to 33 µg/m^3 of $PM_{2.5}$ from TSD area sources, less than 2 µg/m^3 from mobile sources, while the point sources in the region contributed up to 13 µg/m^3.

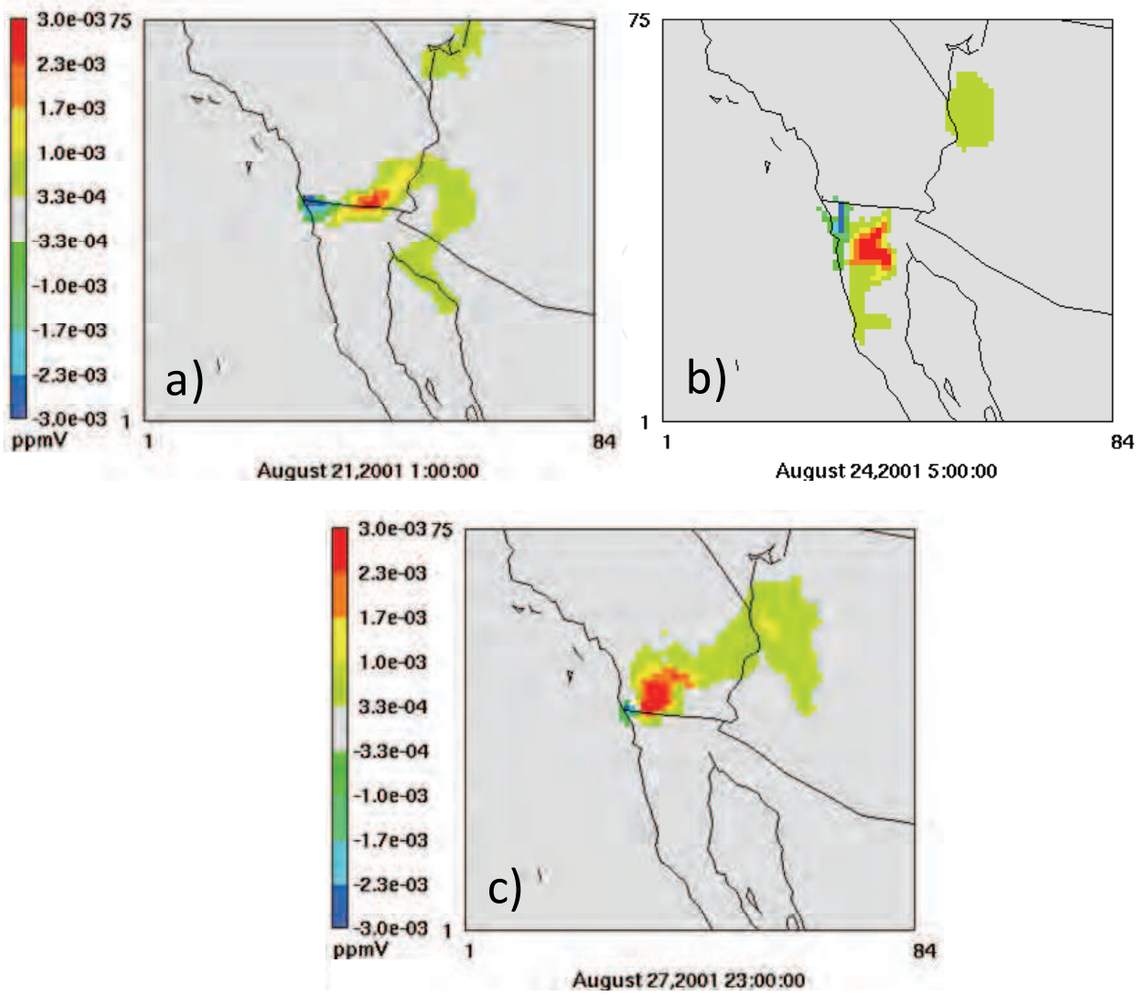

Fig. 19. O_3 sensitivity to Tijuana mobile sources during the August 2001 episode (see text for details).

4.3.3 Source contribution during the winter episode

Contributions to O_3 from various sources in the region were simulated for the winter episode. Impact of LAR mobile sources of up to 14 ppbv was seen over the Pacific Ocean. High contributions were also observed along the coast from Los Angeles to San Diego, which represents a major travel road route (Figure 21a). MXC area sources had simulated impacts of up to 6 ppbv over the southern regions of Baja California.

However, much of the time fresh NOx emissions led to decreases (negative sensitivities) over the local urban areas and positive impacts downwind. Peak impacts of 11 ppbv of O_3 were simulated over the Los Angeles area during the winter episode which originate from TSD area sources (Figure 21b). This same changes originated O_3 reductions of more than 7 ppbv over TSD.

Similar values as that in summer episode were simulated with peak impacts of up 2 ppbv O_3 on the Baja California region from Mexicali mobile emissions. Tijuana, San Diego and Calexico mobile sources contribute to less than 6 ppbv O_3 during the winter episode.

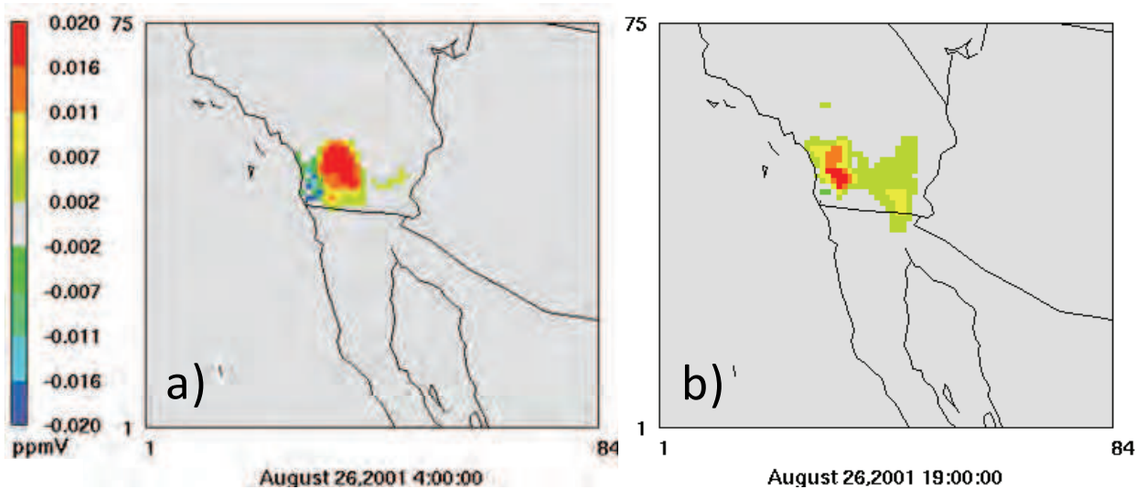

Fig. 20. O_3 sensitivity to San Diego mobile sources during the August 2001 episode (see text for details).

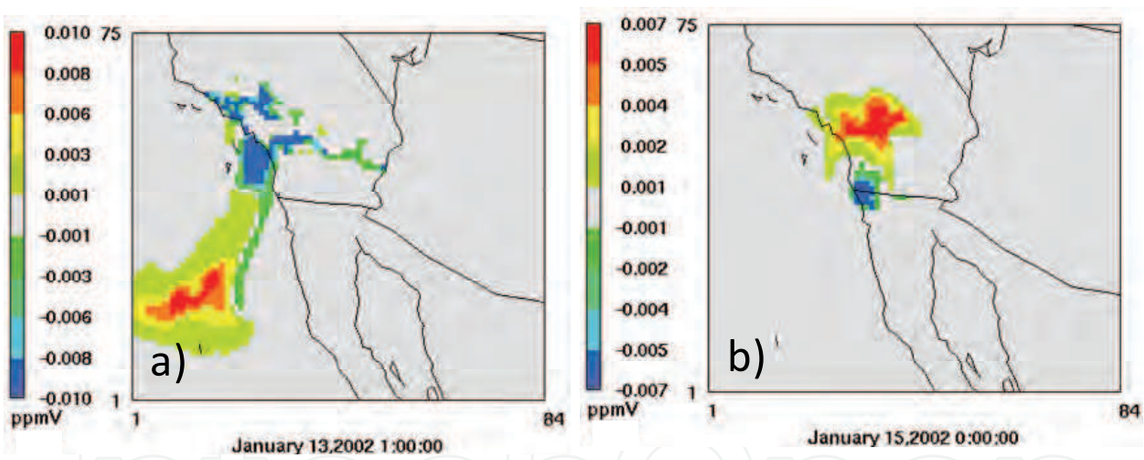

Fig. 21. Peak O_3 sensitivity to (a) LAR mobile sources and (b) to TSD area sources, during the January 2002 episode.

MXC area sources contribute to a simulated $PM_{2.5}$ maximum of 34 μg/m³ (Figure 22a). The pattern is very localized. Primary $PM_{2.5}$ emissions from MXC mobile sources contribute negligibly with peak contributions of 0.5 μg/m³. MXC point sources, primarily present in Mexicali contributed to a maximum of 12 μg/m³ over the border region. Area sources in TSD had very large contributions, ranging up to 52 μg/m³ (Figure 22b). However, once again the extent of the sensitivity field is constrained to the vecinitiy of the cities of Tijuana and San Diego. TSD mobile sources contributed to less than 3 μg/m³ of primary $PM_{2.5}$. Point sources in San Diego contributed to a maximum 13 μg/m³ of primary $PM_{2.5}$ in the region.

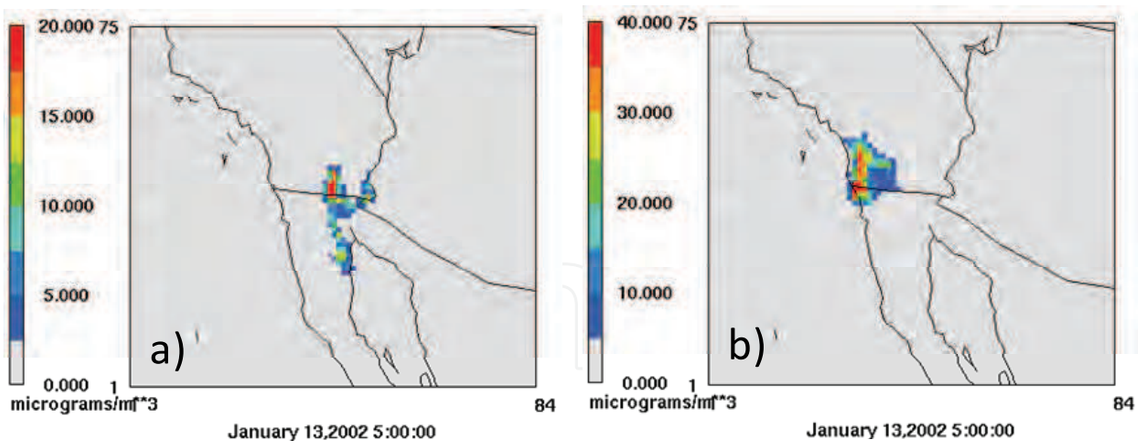

Fig. 22. Peak contribution to $PM_{2.5}$ from (a) MXC primary $PM_{2.5}$ area sources and (b) TSD primary $PM_{2.5}$ area sources, during the January 2002 episode.

5. Conclusion

Results suggest relevant information on trans-boundary impacts of air pollutants in the Mexicali-Imperial Valley border area. Simulated O_3 and $PM_{2.5}$ concentrations in the domain were the highest in the LA area, as expected. However, limited contribution of sources in the LAR area to O_3 and $PM_{2.5}$ levels in the border region was observed. Mobile sources, the most abundant sources in the LAR area contributed up to 10 ppbv of O_3 in MXC, but meteorological events that favored the transport of pollutants from LAR to MXC were few compared to prevailing conditions that favored transport to the east and northeast of LAR during the summer episodes or the southwest during the winter episode. Emissions from the TSD region play a much more important role in the air quality of the MXC area, particularly on the levels of O_3 during the summer episodes. Again, mobile sources contributed the most to the observed impacts from TSD to MXC. Even more, MXC O_3 levels were more sensitive to NOx changes in TSD mobile emissions than VOC changes in that same source. Even though, mobile sources are of concern in the MXC area, O_3 impacts from precursors emitted within the region were small. Area sources in MXC contributed the most: up to a maximum of 8 ppbv of O_3 during the summer episodes. O_3 plumes reached the border regions of California-Arizona and O_3 concentrations up to 4 ppbv in the Grand Canyon area can be attributed to area sources in the MXC region. The MXC region is more sensitive to NOx controls than to VOCs controls. In regards to $PM_{2.5}$, about 50% of the $PM_{2.5}$ in MXC during the summer episode can be attributed directly to area sources. During the winter episode, plumes from TSD, LAR and Las Vegas unite and move towards the MXC region with impacts of 10-35 $\mu g/m^3$. Soil dust contribution from LAR, TSD and MXC ranges between 5-25 $\mu g/m^3$. MXC area sources contribute a maximum of 34 $\mu g/m^3$ $PM_{2.5}$.

6. Acknowledgments

This study was supported by LASPAU: Academic and Professional Programs for the Americas, under its Border Ozone Reduction and Air Quality Improvement Program. Additional support was obtained from Tecnológico de Monterrey through grant CAT-186.

7. References

Bergin, M.S.; Shih, J.S.; Krupnick, A.J.; Boylan, J.W.; Wilkinson, J.G.; Odman, M.T. & Russell, A.G. (2007). Regional air quality: Local and interstate impacts of NOx and SO_2 emissions on ozone and fine particulate matter in the Eastern United States. *Environ. Sci. Technol*., 41(13), 4677-4689.

Breiman, L., Friedman, J.; Olshen, R. & Stone, C. (1998) Classification and regression trees. Chapman & Hall/CRC, ISBN 0-412-04841-8, Boca Raton, FL.

Byun, D.W. & Ching, J.K.S. (1999). *Science Algorithms of the EPA Models 3 Community Multiscale Air Quality (CMAQ) Modeling System*. EPA/600/R-99/030, US EPA, Washington DC.

Carter, W.P.L. (2000). *Documentation of the SAPRC99 chemical mechanism for VOC reactivity assessment*. Center for Environmental Research and Technology, University of California, Riverside, CA.

Che, W.; Zheng, J.; Wang, S.; Zhong, L. & Lau, A. (2011). Assessment of motor vehicle emission control policies using Model-3/CMAQ model for the Pearl River Delta region, China. *Atmos. Environ*., 45, 1740-1751.

Choi, Y.-J.; Hyde, P. & Fernando, H.S.J. (2006). Modeling of episodic particulate matter events using a 3-D air quality model with fine grid: Applications to a pair of cities in the US/Mexico border. *Atmos. Environ*., 40, 5181-5201.

Chow, J. C.; Watson, J. G.; Green, M. C.; Lowenthal, D. H.; Bates, B.; Oslund, W. & Torres, G. (2000). Cross-border transport and spatial variability of suspended particles in Mexicali and California's Imperial Valley. *Atmos. Environ*., 34, 1833-1843.

Chow, J.C. & Watson, J.G. (2001). Zones of representation for PM_{10} measurements along the US-Mexico border. *The Sci. of the Total Environ*., 276, 49-68.

Cohan, D. S.; Hakami, A.; Hu, Y. T. & Russell, A. G. (2005). Nonlinear response of ozone to emissions: Source apportionment and sensitivity analysis. *Environ. Sci. Technol*., 39, 6739-6748.

Currey, R.C.; Kelly, K.E.; Meuzelaar, H.L.C. & Sarofim, A.F. Eds. (2005). *The U.S.-Mexican Border Environment: Integrated Approach to Defining Particulate Matter in the Paso del Norte Region*. SCERP Monograph Series, No. 12, San Diego State University Press, ISBN 0-925613-47-9, San Diego, CA.

Deane, M. (1984). Epidemiological monitoring plan for geothermal developments. *Sci. Total Environ*., 32(3), 303-320.

Dennis, R.L.; Mathur, R.; Pleim, J.E. & Walker, J.T. (2010). Fate of ammonia emissions at the local to regional scale as simulated by the Community Multiscale Air Quality model. *Atmos. Pollution Res*., 1, 207-214.

Dunker, A.M. (1984). The Decoupled Direct Method for Calculating Sensitivity Coefficients in Chemical-Kinetics. *Journal of Chemical Physics*, 81, 2385-2393.

Dunker, A.M.; Yarwood, G.; Ortmann, J.P. & Wilson, G.M. (2002). Comparison of source apportionment and source sensitivity of ozone in a three-dimensional air quality model. *Environ. Sci. Technol*., 36, 2953-2964.

Eatough, D. J.; Green, M.; Moran, W. & Farber, R. (2001). Potential particulate impacts at the Grand Canyon from northwestern Mexico. *Sci. Total Environ*., 276, 69-82.

ERG (Eastern Research Group), Acosta y Asociados & TransEngineering. (2004). Mexico National Emissions Inventory, 1999: Six Northern States, Final Report prepared for SEMARNAT, INE, US EPA, WRAP and CEC; Report #3393-00-011-002.

Grell, G.; Dudhia, J. & Stauffer, D.R. (1994). *A description of the Fifth-Generation Penn State/NCAR Mesoscale Model (MM5)*. NCAR Technical Note, NCAR/TN-398+STR.

Gudiksen, P.H.; Ermak, D.L.; Lamson, K.C.; Axelrod,M. C. & Nyholm, R.A. (1980). Potential air quality impact of geothermal power production in the Imperial Valley. *Atmos. Environ*., 14(11), 1321-1330.

Hakami, A.; Odman, M. T. & Russell, A. G. (2003). High-order, direct sensitivity analysis of multidimensional air quality models. *Environ. Sci. Technol*., 37, 2442-2452.

Hakami, A.; Odman, M.T. & Russell A.G. (2004). Nonlinearity in atmospheric response: A direct sensitivity analysis approach. *J. Geophys. Res*., 109 (D15), D15303.

Houyoux, M.R. & Vukovich, J.M. (1999) Updates to the Sparse Matrix Operator Kernel Emissions (SMOKE) Modeling System and Integration with Models-3. *Conference The Emission Inventory: Regional Strategies for the Future*, Air & Waste Manage. Assoc., Raleigh, NC.

Im, U.; Poupkou, A.; Incecik, S.; Markakis, K.; Kindap, T.; Unal, A.; Melas, D.; Yenigun, O.; Topcu, S.; Odman, M.T.; Tayanc, M. & Guler, M. (2011). The impact of anthropogenic and biogenic emissions on surface ozone concentrations in Istanbul. *Sci. Total Environ*., 409, 1255-1265.

Kelly, K.E.; Jaramillo, I.C.; Quintero-Núñez, M.; Wagner, D.A.; Collins, K.; Meuzelaar, H.L.C. & Lighty, J.S. (2010). Low-Wind/High Particulate Matter Episodes in the Calexico/Mexicali Region. *J. Air & Waste Manage. Assoc*., 60, 1476-1486.

Kenski, D.M. (2004). CART Analysis of Historic Ozone Episodes. In *Proceedings of the AWMA 97th Annual Conference and Exhibition*, Indianapolis, USA.

Liao, K.-J.; Tagaris, E.; Manomaiphiboon, K.; Napelenok, S.L.; Woo, J.-H.; He, S.; Amar, P. & Russell, A.G. (2007). Sensitivities of Ozone and Fine Particulate Matter Formation to Emissions under the Impact of Potential Future Climate Change. *Environ. Sci. Technol*., 41, 8355-8361.

McMurry, P.; Sheperd, M. & Vickery, J. (Eds.) (2004) *Particulate Matter Science for Policy Makers: A NARSTO Assessment*, Cambridge University Press, ISBN 0-521-84287-5, New York, USA.

Mendoza-Dominguez, A.; Wilkinson, J. G.; Yang, Y.-J. & Russell, A. G. (2000). Modeling and Direct Sensitivity Analysis of Biogenic Emissions Impacts on Regional Ozone Formation in the Mexico-U.S. Border Area. *J. Air & Waste Manage. Assoc*., 50, 21-31.

Mendoza, A.; Gutiérrez, A.A. & Pardo, E.I. (2009). Volatile organic compounds in the downtown area of Mexicali, Mexico during the spring of 2005: analysis of ambient data and source-receptor modeling. *Atmósfera*, 22, 195-217.

Mendoza, A.; Pardo, E.I. & Gutierrez, A.A. (2010). Chemical Characterization and Preliminary Source Contribution of Fine Particulate Matter in the Mexicali/Imperial Valley Border Area. *J. Air & Waste Manage. Assoc*., 60, 258-270.

Morris, R.E.; Koo, B.; Lau, S.; Tesche, T.W.; McNally, D.; Loomis, C.; Stella, G.; Tonnesen, G. & Wang, Z. (2004). *VISTAS Emissions and Air Quality Modeling – Task 4: Model Performance Evaluation and Model Sensitivity Tests for Three Phase I Episodes*. Report prepared by ENVIRON International Corporation, Novato, California.

Mukerjee, S. (2001). Selected air quality trends and recent air pollution investigations in the US-Mexico border region. *Sci. Total Environ*., 276, 1-18.

Olerud, D. & Sims, A. (2003). *MM5 sensitivity modeling in support of VISTAS (Visibility Improvement – State and Tribal Association*. Report prepared for the VISTAS Technical Analysis Workgroup by Baron Advanced Meteorological Systems, LLC.

Osornio-Vargas, A.R.; Hernandez-Rodriguez, N.A.; Yanez-Buruel, A.G.; Ussler, W.; Overby, L.H.; Brody, A.R. (1991) Lung cell toxicity experimentally induced by a mixed dust from Mexicali, Baja California, Mexico. *Environ. Res.*, 56(1), 31-47.

Pitchford, M.L.; Tombach, I., Barna, M.; Gebhart, K.A.; Green, M.C.; Knipping, E.; Kumar, N.; Malm, W.C.; Pun, B.; Schichtel, B.A.; Seigneur, C. (2004). *Big Bend Regional Aesorol and Visibility Observational Study (BRAVO) Final Report*, September 2004.

Quintero-Núñez, M.; Reyna, M.A.; Collins, K.; Guzmán, S.; Powers, B. & Mendoza, A. (2006). Issues Related to Air Quality and Health in the California-Baja California Border Region, In *The U.S. Mexican border environment: Binational Air Quality Management*, SCERP Monograph Series No. 14, R. Pumfrey (Ed.), 1-46, San Diego State University Press, ISBN: 0-925613-50-9, San Diego, California, USA.

Russell, A. & Dennis, R. (2000). NARSTO critical review of photochemical models and modeling. *Atmos. Environ*., 34, 2283-2324.

Russell, A.G. (2008). EPA Supersites Program-Related Emissions-Based Particulate Matter Modeling: Initial Applications and Advances. *J. Air & Waste Manage. Assoc*., 58, 289-302.

Sheya, S.A.N.; Meuzelaar, H.L.C.; Jeon, S.J.; Dworzanski, J.P.; Jarman, W.; Kasteler, C.; Lighty J.; Sarofim, A.; Li, W.W.; Valenzuela, V.; Anderson, J.; Banerji, S.; Perry, D.; Mejia, G.; Zavala, M. & Simoneit, B. (2000) Novel Analytical Dimensions in Exploratory Field Studies of Air Particulate Matter, *Proceedings of the 93rd Air & Waste Management Association's Annual Conference & Exhibition*, pp. 1104-1130, Salt Lake City, UT, USA, June 18-22, 2000.

Sweedler, A.; Fertig, M.; Collins, K. & Quintero-Núñez, M. (2003). Air Quality in the California-Baja California Border Region, In *The U.S. Mexican border environment: Air Quality Issues along the US-Mexico Border*, SCERP Monograph Series No. 6, A. Sweedler (Ed.), 15-58, San Diego State University Press, ISBN: 0-925613-38-X, San Diego, California, USA.

Tagaris, E.; Manomaiphiboon, K.; Liao, K.-J.; Leung, L.R.; Woo, J.-H.; He, S.; Amar, P. & Russell, A.G. (2007). Impacts of global climate change and emissions on regional ozone and fine particulate matter concentrations over the United States. *J. Geophys. Res*., 112(D14), D14312/1-D14312/11.

Tesche, T.W.; Georgopoulos, P.; Seinfeld, J.H.; Cass, G.; Lurmann, F.L. & Roth, P.M. (1990). *Improvement of procedures for evaluating photochemical models*, Report prepared by Radian Corporation for the State of California Air Resources Board, Sacramento, CA.

US EPA. (2003) *User's Guide to Mobile6.1 and Mobile6.2 Mobile Source Emission Factor Model*. Office of Transportation and Air Quality, EPA420-R-03-010, Ann Arbor, MI.

Vanoye, A.Y. & Mendoza, A. (2009). Mesoscale Meteorological Simulations of Summer Ozone Episodes in Mexicali and Monterrey, Mexico: Analysis of Model Sensitivity to Grid Resolution and Parameterization Schemes. *Water, Air, & Soil Pollution: Focus*, 9, 185-202.

Vukovich, J. & Pierce, T. (2002). The Implementation of BEIS3 within the SMOKE Modeling Framework. *United States Environmental Protection Agency Emissions Inventory Conference*, Atlanta, GA.

Yang, Y. J.; Wilkinson, J.G. & Russell, A.G. (1997). Fast, direct sensitivity analysis of multidimensional photochemical models. *Environ. Sci. Technol*., 31, 2859-2868.

Ying, Q. & Krishnan, A. (2010). Source contributions of volatile organic compounds to ozone formation in southeast Texas. *J. Geophys. Res*., 115(D17), D17306/1-D17306/14.

Watson, J.G. & Chow, J.C. (2001). Source characterization of major emission sources in the Imperial and Mexicali Valleys along the US/Mexico border. *Sci. Total Environ*., 276, 33-47.

Zavala, M.; Herndon, S.C.; Wood, E.C.; Jayne, J.T.; Nelson, D.D.; Trimborn, A.M.; Dunlea, E.; Knighton, W.B.; Mendoza, A.; Allen, D.T.; Kolb, C.E.; Molina, M.J. & Molina, L.T. (2009). Comparison of emissions from on-road sources using a mobile laboratory under various driving and operational sampling modes. *Atmos. Chem. Phys*., 9, 1-14.

Zielinska, B.; Sagebiel, J.; Harshfield, G. & Pasek, R. (2001). Volatile organic compound measurements in the California-Mexico border region during SCOS97. *The Sci. of the Total Environ*., 276, 19-31.

Zuk M.; Rojas Bracho, L. & Tzintzun Cervantes, M.G. (2007). *Tercer almanaque de datos y tendencias de la calidad del aire en nueve ciudades mexicanas*. Instituto Nacional de Ecología, ISBN 978-968-817-840-9, México, D.F.

Advanced Air Pollution

Edited by Dr. Farhad Nejadkoorki

ISBN 978-953-307-511-2
Hard cover, 584 pages
Publisher InTech
Published online 17, August, 2011
Published in print edition August, 2011

Leading air quality professionals describe different aspects of air pollution. The book presents information on four broad areas of interest in the air pollution field; the air pollution monitoring; air quality modeling; the GIS techniques to manage air quality; the new approaches to manage air quality. This book fulfills the need on the latest concepts of air pollution science and provides comprehensive information on all relevant components relating to air pollution issues in urban areas and industries. The book is suitable for a variety of scientists who wish to follow application of the theory in practice in air pollution. Known for its broad case studies, the book emphasizes an insightful of the connection between sources and control of air pollution, rather than being a simple manual on the subject.

InTech Europe
University Campus STeP Ri
Slavka Krautzeka 83/A
51000 Rijeka, Croatia
Phone: +385 (51) 770 447
Fax: +385 (51) 686 166
www.intechopen.com

InTech China
Unit 405, Office Block, Hotel Equatorial Shanghai
No.65, Yan An Road (West), Shanghai, 200040, China
中国上海市延安西路65号上海国际贵都大饭店办公楼405单元
Phone: +86-21-62489820
Fax: +86-21-62489821

IntechOpen